



# The effect of the source and the concentration of polymers on the release of chlorhexidine from mucoadhesive buccal tablets

Enas Al-Ani<sup>a,b,\*</sup>, Claire Martin<sup>c</sup>, Stephen T. Britland<sup>d</sup>, Khalid Doudin<sup>e</sup>, David J. Hill<sup>b,f,\*</sup>

<sup>a</sup> School of Pharmacy, Faculty of Science and Engineering, University of Wolverhampton, Wolverhampton, UK

<sup>b</sup> Research Institute in Healthcare Science, Faculty of Science and Engineering, University of Wolverhampton, Wolverhampton, UK

<sup>c</sup> Department of Biological Sciences, Institute of Science and the Environment, University of Worcester, Worcester, UK

<sup>d</sup> School of Health Sciences, York St John University, York, UK

<sup>e</sup> Chemical Engineering and Applied Chemistry, Aston University, Birmingham, UK

<sup>f</sup> School of School of Biology, Chemistry and Forensic Science, Faculty of Science and Engineering, University of Wolverhampton, Wolverhampton, UK

## ARTICLE INFO

### Article history:

Received 21 December 2018

Accepted 19 April 2019

Available online 20 April 2019

### Keywords:

Buccal tablet

Mucoadhesion

Particle morphology

Poloxamer 407

Hydroxypropyl methylcellulose

Chlorhexidine

Surfactant polymer

## ABSTRACT

In the current work, two groups of chlorhexidine mucoadhesive buccal tablets were prepared, using either rod or irregularly-shaped spherical particles of hydroxypropyl methylcellulose and different ratios of poloxamer 407 (P407). The tablets were designed to release the drug over two hours. Their physico-chemical properties and drug release profiles were investigated. The impact on dry granulation, the *ex-vivo* mucoadhesion, the swelling index, the morphology of swollen tablets and the drug release kinetic were investigated. Drug-polymers chemical interaction was studied using Fourier Transforms Infrared Spectroscopy (FTIR) and differential scanning calorimetry (DSC). Due to different particle shapes, the preparation of dry granules required a 40 KN force for rod-shaped particles compared to 10 KN for the irregularly-shaped spherical particles. All formulations showed at least two-hours residence time using *ex-vivo* mucoadhesion. Statistically, there was no significant difference in the swelling index, drug release nor its kinetic for both groups. However, the microscopical morphology of the swollen tablet and the size of the pores were affected by particle shape. Increasing the ratio of P407 to 62.5% resulted in a pronounced increase in drug release from around 60% to >90% after two hours. Following the FTIR and DSC analyses, no chemical interaction was noted apart from the steric hindrance effect of P407, which was observed even with the physical mixtures.

© 2019 Production and hosting by Elsevier B.V. on behalf of King Saud University. This is an open access article under the CC BY-NC-ND license (<http://creativecommons.org/licenses/by-nc-nd/4.0/>).

## 1. Introduction

Hydroxypropyl methylcellulose (HM) has widely been used in the preparation of hydrophilic controlled release matrices due to its water solubility, pH stability and resistance to enzymatic degradation, ease of manufacturing and low cost. It gels and swells upon contact with water forming a gelatinous layer that controls drug release (Ghori and Conway, 2015; Maderuelo et al., 2011). Due to its mucoadhesive and hydrogel-forming properties, it has been

\* Corresponding authors at: Faculty of Science and Engineering, University of Wolverhampton, Wulfruna Street, Wolverhampton WV1 1LY, UK.

E-mail addresses: [E.Al-Ani2@wlv.ac.uk](mailto:E.Al-Ani2@wlv.ac.uk) (E. Al-Ani), [D.Hill@wlv.ac.uk](mailto:D.Hill@wlv.ac.uk) (D.J. Hill).

Peer review under responsibility of King Saud University.



investigated in buccal drug delivery and is included in marketed products (Sudhakar et al., 2006). There are several factors which affect drug release from HM matrices, for instance, particle size (Wan et al., 2001), force of compression (Velasco et al., 1999), molecular weight (Gao et al., 1996), viscosity (Campos-Aldrete, 1997), drug polymer ratio (Velasco et al., 1999), and the incorporation of other polymers or excipients (Xie et al., 2017). There have been only a limited number of investigations which have highlighted the effect of particle shape on tablet swelling and drug release. For instance, Gustafsson et al. (1999) assumed that fibrous or rod-shaped HM particles have a lower hydration rate compared to irregular particles, which results in a lower gelling rate and consequently decreases the rate of drug release. Moreover, the morphology of the powder affects its flow properties and compactability. Rod-shaped interlocked upon compaction and produced higher tensile strength tablets, which consequently resulted in a decreased drug release rate (Gustafsson et al., 2003). Li et al. (2005) found that the rod-shaped particles in Methocel powder

also interlocked, producing a stronger matrix which affected tablet swelling and decreased the rate of drug release.

Poloxamer 407 (P407) or Pluronic F127 is a non-ionic surfactant polymer and has a thermo-reversible hydrogel-forming ability with a mucoadhesive property. It gels at a concentration of >20% at 25 °C (Ruel-Gariépy and Leroux, 2004). It is a copolymer of polyethylene oxide and polypropylene oxide, with the hydrophilic nature of the former and the hydrophobic nature of the latter resulting in an amphiphilic molecule with consequent surfactant properties (Kabanov et al., 2002). It has a wide application in drug delivery, for example, in parenteral, ophthalmic, inhaler, oral solution, suspension, and topical formulations (Dumortier et al., 2006). In the current work, P407 was chosen due to its pronounced gelling properties and high viscosity of 3100 cP which is attributed to its high molecular weight compared to other poloxamers and its availability as microprills (Matanovi et al., 2014). Although, it is not commonly used in controlling the release of the drug from solid dosage forms, in the current work it was formulated in tablet dosage form to control the release of chlorhexidine (CHD) together with HM by exploiting its thermo-reversible hydrogel-forming properties which promotes tablet wetting as a result of its surfactant property.

CHD is cationic at physiologic pH, its bactericidal and fungicidal activity results from its ability to bind to phosphate-containing proteins in the bacterial or fungal cell walls and membranes which leads to structural disruptions and leakage of cytoplasmic components (Lim and Kam, 2008). The main advantage of oral formulations of CHD is their lack of a specific cellular target for microbiocidal activity which results in the retardation of the development of resistance against CHD (Ankola et al., 2008). CHD mouthwashes are prescribed as adjuvant for the treatment of oropharyngeal candidiasis (OPC) (Pereiro Ferreirós et al., 2012). The greatest disadvantage of current CHD formulations is their short retention and activity time in the oral cavity. Consequently, there is a real need for a new approach to the localised, prolonged delivery of antifungal agents for enhanced OPC therapy. The advantages of this mode of drug delivery are that it reduces the systemic side effects of the drug, minimizes the dose of the drug required and provides targeted drug delivery (Sankar et al., 2011).

In the present study, the impact of HM particle shape and/or the ratio of P407 on the properties and the release of CHD from mucoadhesive matrices are investigated. To the best of our knowledge, there has been no previous investigation into the impact of the shape of HM particles on tablet behaviour and release profile, after being dry granulated. The effects on the physicochemical properties of CHD matrix tablets for local oral drug delivery of HM rod and irregularly-shaped spherical particles were studied. The tablets were designed to control the release for two hours which might not be achieved by HM. Accordingly, P407 was added to increase the hydrophilicity and maintain the hydrogel network structure. The effect of P407 on tablet behaviour and the CHD release profile was investigated.

## 2. Materials and method

### 2.1. Materials

Methocel™ F4M premium hydroxypropyl methylcellulose (Methocel, viscosity of 2663–4970 cps for 2% solution at 20 °C, 27–30% methoxyl and 4–7.5% hydroxypropyl substitution) was kindly donated by the Dow-Colorcon Company in the U.K. Hydroxypropyl methylcellulose (HPMC, Mn ~ 86,000, viscosity of 4000 cps for 2% solution at 20 °C, 29% methoxyl and 7% hydroxypropyl substitution), poloxamer 407 (P407) and chlorhexidine diacetate salt hydrate (CHD) were purchased from Sigma Aldrich in the UK and Magnesium stearate from Alfa Aesar, also in the UK.

### 2.2. Solubility of CHD

The solubility of CHD was investigated in ultra-pure water and a phosphate buffer saline (PBS) solution pH 6.8, as a simulated salivary pH to select the most appropriate dissolution medium with a sink condition.

The solubility of CHD was determined by adding excess CHD to 3 mL of water or a PBS solution at pH 6.8. The samples were shaken at  $37 \pm 0.1$  °C for 24 h. The suspensions were filtered through a 0.45 µm Millipore membrane filter and the concentration of CHD was measured by UV detection at  $\lambda_{254}$  nm (Biochrom WPA Bio-wave II UV-Spectrophotometry, UK).

### 2.3. Particle size and morphological analyses

The raw materials were assessed for their size. The volume-weighted particle size of Methocel, HPMC, P407 and CHD was assessed by laser diffraction using a Malvern Mastersizer 3000 with an Aero S dry dispersion unit system (Malvern Instruments, Malvern, UK). The cumulative particle sizes at 10, 50 and 90% were displayed as  $D_{0.1}$ ,  $D_{0.5}$  and  $D_{0.9}$ , respectively.

The morphology of the granules and the raw materials was assessed by scanning using electron microscopy (SEM), (Zeiss Evo® 50EP SEM, Germany).

### 2.4. Preparation of tablets using the dry granulation technique

The formulations of CHD mucoadhesive tablets were prepared as shown in Table 1. The powders were blended for 5 min in a V-shaped powder blender (CapsulCN®, China). Then, dry granules were prepared following the slugging method (Tuğcu-Demiröz et al., 2004) using a manual hydraulic hand press (diameter = 4 cm, weight =  $5.5 \pm 0.5$  g). Slugs prepared using HPMC and Methocel were formed with a compression force of 10 and 40 KN, respectively. The slugs were crushed into granules and passed through a 1 mm screen (mesh no. 18). Magnesium stearate (0.5%) was added and mixed for 3 min prior to the compression of the granules into tablets.

The tablets were pressed using a heavy duty mini rotary tablet machine (STC ZPS Shanghai, China) with a biconvex 6 mm diameter round shape punch. The average central thickness was 1.5 mm and the wall thickness (edge) was 1.0 mm.

### 2.5. Flow properties and compressibility index

The bulk and the tapped volume of the powder blends and the granules were assessed using a tapped Density tester (Varian, UK). The tapped volumes were obtained by subjecting the powders to 200 taps each time until a constant volume was achieved. Carr's Compressibility index (CI) was calculated using the flowing equation

$$\text{Carr's Index} = (1 - V_t/V_0)$$

where  $V_0$  is bulk volume and  $V_t$  is the tapped volume.

### 2.6. Characterisation of the buccal tablets

#### 2.6.1. Friability and tensile strength

A sample of approximately 1 g of each formulation was evaluated for their friability using a friability tester (Charles Ischi AG, AE-1, UK), and rotated 100 times at 25 rpm. The mechanical strength of the biconvex tablet was calculated using the following equation (Pitt et al., 1988).

$$\sigma_x = 10F/\pi D^2 [2.84H/D - 0.126H/W + 3.15W/D + 0.01]^{-1}$$

**Table 1**  
Formulations of CHD mucoadhesive buccal tablets.

Formulations	Weight (mg)/tablet				Tablet weight
	CHD	HPMC	Methocel	P407	
F1	5	25.0	–	–	30
F2	–	20.5	–	4.5	–
F3	–	17.5	–	7.5	–
F4	–	11.5	–	13.5	–
F5	–	6.25	–	18.75	–
F6	–	–	25.0	–	–
F7	–	–	20.5	4.5	–
F8	–	–	17.5	7.5	–
F9	–	–	11.5	13.5	–
F10	–	–	6.25	18.75	–

where  $\sigma_x$  is the tensile strength,  $F$  is tablet hardness (Newtons),  $D$  is tablet diameter,  $H$  is tablet thickness, and  $W$  is central cylinder thickness (tablet wall height), with all tablet dimensions in mm.

Tablet hardness was measured using a Varian VK 200, (UK) hardness tester ( $n = 10$ ).

#### 2.6.2. Ex-vivo mucoadhesion analysis

The mucoadhesion was determined as a function of dosage form residence time using a modified protocol adopted from Nafee et al. (2003). Freshly harvested chicken crops were carefully washed to remove any residue of food the chicken had consumed, and they were subsequently stored at  $-80^\circ\text{C}$ . The crops were defrosted before use, cut into small pieces ( $1\text{ cm} \times 2\text{ cm}$ ) and fixed to a glass slide using cyanoacrylate glue. The crop was hydrated using one drop of ultrapure water before a CHD tablet was placed on top and weighed down with a 4 g weight for 20 s to aid the adhesion process. The glass slide was then placed into the disintegration apparatus tubes (cylinders) (Varian VK 100, UK), prefilled with  $37 \pm 0.2^\circ\text{C}$  of ultrapure water (Fig. 1). A test, similar to the disintegration test, was performed at 50 rpm for 120 min with periodic sample examination for every 15 min to evaluate if the tablets had become detached from the chicken crops. The formulation of each tablet was performed in triplicate.

#### 2.6.3. Swelling index

The swelling index was determined by weighing an individual CHD tablet ( $W_0$ ) and sticking it to a previously weighed glass coverslip using a single water droplet and allowing it to equilibrate for 30 s. The coverslip was then placed vertically in a beaker in a  $37 \pm 0.2^\circ\text{C}$  water bath (Clifton, Nickel-Electro Ltd, UK). The weight of the swollen tablet ( $W_s$ ) was recorded at 30, 60, 90 and 120 min. The swelling index (SI) was calculated using the following equation (Kassem et al., 2014).

$$SI = (W_s - W_0)/W_0$$

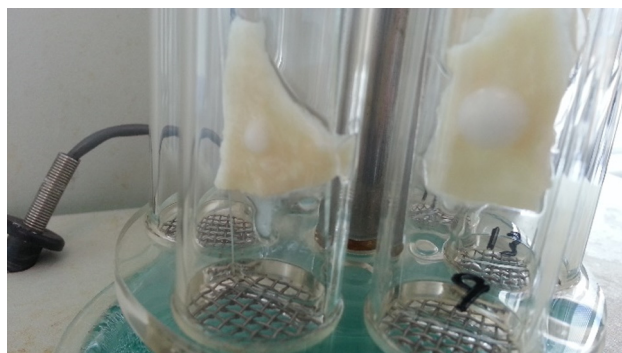


**Fig. 1.** Ex-vivo mucoadhesion using the disintegration apparatus.

#### 2.6.4. Tablet morphology (SEM)

The morphology of aqueous media swollen tablets was investigated. They were prepared by adding 0.5 mL distilled water to each tablet in a 5 mL test tube and left until swollen. They were then freeze-dried using a Beta 1–8 LSC Freeze Dryer (Christ, UK). The tablets were cut in half and analysed using SEM as previously described. The surface area of the pores was measured using ImageJ 1.51n software.

**2.6.4.1. Comparison of dissolution rate.** Similarity and difference factors were applied to compare the dissolution profiles of both groups of formulations. The similarity factor ( $f_2$ ) was calculated using the equation below. The results fell between 0 and 100%, and an  $f_2$  of  $\geq 50$  suggests a similarity between the standard and the test (Costa and Lobo, 2001).

$$f_2 = 50 \times \log \left\{ \left[ 1 + (1/n) \sum_{t=1}^n (R_t - T_t)^2 \right]^{-0.5} \times 100 \right\}$$

where  $n$  is the number of time points,  $R_t$  is the percent release of the standard and  $T_t$  is the percent release of the test.

The difference factor ( $f_1$ ) was calculated using the equation below. Values of between 0 and 15 indicate that the difference between the samples is acceptable. When  $f_1 = 0$ , the two samples are considered identical (Costa and Lobo, 2001).

$$f_1 = \left\{ \left[ \sum_{t=1}^n |R_t - T_t| \right] / \left[ \sum_{t=1}^n (R_t + T_t)/2 \right] \right\} \times 100$$

#### 2.6.5. In-vitro dissolution of CHD (Apparatus I)

The dissolution was performed using Varian 705 DS BP Dissolution Apparatus type I (basket method) (Varian, UK). One tablet of each formulation was placed in 500 mL of ultrapure distilled water at  $37 \pm 0.1^\circ\text{C}$ , with the basket rotating at  $50 \pm 1$  rpm. At predetermined time intervals, 4 mL was withdrawn from the dissolution medium and replaced with the same volume of fresh media. The CHD concentration was determined spectrophotometrically at  $\lambda_{254}$  (Biochrom WPA Biowave II UV-Spectrophotometry, UK).

**2.6.5.1. Kinetics of drug release.** The kinetics of CHD release were investigated to further understand the mechanism of CHD release and the effect of the different ratios of the polymers. Five models (Costa and Lobo, 2001) were used to analyse the release of CHD from the tablet matrices (Table 2).

#### 2.7. Fourier transform Infrared Spectroscopy (FTIR) and differential scanning calorimetry (DSC)

FTIR was used to investigate the possibility of interaction between the polymers and CHD. Spectra were obtained using a Bruker Alpha spectrometer (Germany) scanning and ranged from  $4000$  to  $400\text{ cm}^{-1}$ .

**Table 2**  
Kinetic drug release models.

Model	Equation
Zero order	$Q = Q_0 - K_0t$
First order	$\log Q = \log Q_0 - K_1t/2.303$
Higuchi	$Q_t = K_H t^{1/2}$
Hixon-Crowell	$Q^{1/3} = Q_0^{1/3} - K_c t$
Korsmeyer-Peppas	$Q_t/Q_\infty = Kt^n$

Where  $Q$  is the amount of drug released or dissolved at time  $t$ ;  $Q_0$  is the amount of drug release or dissolved at time  $t$  (usually  $t = 0$ );  $Q_t/Q_\infty$  is the fraction of drug released at time  $t$ ;  $K$  is constant, and  $n$  indicates the release mechanism.

DSC analysis was performed to investigate the interaction between CHD and the polymers during the processing steps. Samples of  $5.0 \pm 0.2$  mg each of CHD, HPMC, P407, F10 Physical mix, F10 granules and F10 tablet were investigated. Each was heated in an aluminium pan under a nitrogen flow of 40 mL/min from 25 °C to 300 °C at a scan rate of 10 °C/min. The analysis was performed using Mettler Toledo DSC823e (Switzerland).

### 3. Results and discussion

#### 3.1. Solubility of CHD

The solubility of CHD was investigated to determine the most appropriate dissolution medium to achieve sink condition. Its solubility in water and phosphate buffer saline (PBS) at pH 6.8 was  $23.069 \pm 1.928$  and  $0.047 \pm 0.0124$  mg/mL, respectively. The volume of the dissolution media should be at least 3–10 times that of the saturated volume (Rohrs, 2001). Simulated pH saliva using PBS did not achieve sink condition, which is an important criterion in dissolution. Water showed more than 10 times the saturated volume and was therefore selected as the dissolution medium.

#### 3.2. Particle size and morphology

The particle sizes of CHD and their distribution and excipients are shown in Fig. 2 and Table 3. Both Methocel and HPMC have larger particles than CHD and P407, which is confirmed by the SEM micrographs (Fig. 3).

The SEM micrographs (Fig. 3) correspond with the laser diffraction results. Both CHD and P407 have smaller particle sizes and the latter tend to be more spherical. However, HPMC and Methocel possess larger particle sizes with irregular spherical and rod shapes, respectively.

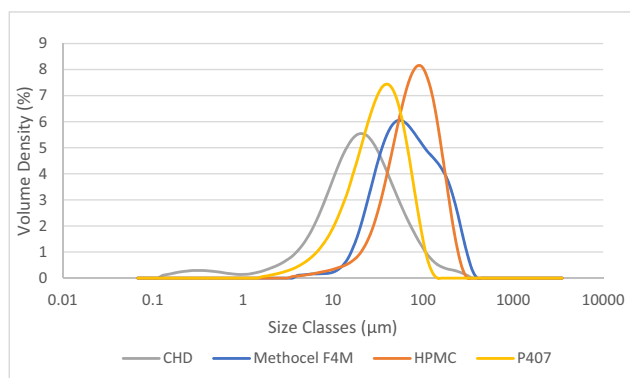


**Fig. 2.** Particle size distribution of CHD, Methocel F4M, HPMC and P407.

Particle size analysis of Methocel showed a broadening of the distribution peak and a higher span value compared to HPMC (Fig. 2) which can be attributed to the rod-like shape of the particles seen under SEM (Fig. 3) (Naito et al., 1998). The particle size distribution of HPMC approximates to a nearly normal distribution pattern with SEM revealing more spherical or irregular spheres.

#### 3.3. Effect of particle morphology on tablet preparation

The morphology of both the HPMC and Methocel samples (Fig. 3) strongly influenced their flow behaviour. HPMC displays a “passable” powder flow (CI of 21.67), whereas Methocel has “poor” flow (CI of 33.33) (British Pharmacopoeia Commission, 2017). This finding was not unexpected as Hassan and Lau (2009) had reported the impeded flow of needle-shaped calcium carbonate particles (CI of  $\approx 40$ ) which resulted from inter-particulate interactions and aggregation. Moreover, the span value of Methocel is higher than HPMC which resulted in a decrease in the flowability. This confirms a previous finding by Liu et al. (2008), who found that the flowability is affected by both particle size and distribution. A particle size of below 100  $\mu\text{m}$  resulted in increased cohesiveness and decreased flowability (Table 3) (Liu et al., 2008), whereas a narrower distribution indicated better flowability. The various powder formulation blends were found not to be flowable (Table 4) and this may be due to the smaller mean particle size population of the formulations, resulting in a relatively high surface area and the potential for increased inter-particulate interactions which can decrease flowability. Dry granulation improved the flow properties of all formulation blends with most improving from ‘very, very poor’ to ‘very poor’, or from ‘very poor’ to ‘poor’ based on the British Pharmacopoeia.

The applied force used to prepare the HPMC granules was 10 KN. In contrast, Methocel granules were initially prepared at 10 and 40 KN, but the 10 KN samples were rejected due to no improvement in flowability. This may be attributed to the rod-like shape of Methocel particulates, which results in weak granules compact which is unable to maintain its shape. The flowability of granulated formulations of HPMC and Methocel prepared by both forces (10 or 40 KN) was similar. Increasing the P407 content decreased the flowability of the powder blends, most likely because of the irregular shape, small particle size and cohesive properties of P407, which increases inter-particulate interactions and decreases packing efficiency as evidenced by a relatively high CI of 40 (Garg et al., 2018). Again, flow properties were improved after granulation, possibly as a result of the low melting point and the waxy nature of the P407, which may have decreased inter-particulate interactions and improved the packing efficiency. Granulated formulations with a high P407 ratio had a CI of 27. The SEM images confirmed that there was no great improvement in the flowability of granules (Fig. 4) due to the generation of fine particles when using dry granulation (Herting and Kleinebudde, 2007).

#### 3.4. Tensile strength and friability

All the tablets showed a tensile strength of less than 1 MP, with Methocel formulations showing relatively higher tensile strengths than HPMC formulations. This might be due to the higher force used in the granulation for the former. All had acceptable levels of friability of less than 1% (Table 5).

#### 3.5. Ex-vivo mucoadhesion

Tablets were prepared with a convex surface. The advantage of this type of surface is that it prevents the tablet from dislodging due to movement of the mouth and reduces contact with the tongue and the teeth (Maurya et al., 2010). It makes the tablet less

**Table 3**  
Particle size distribution of CHD, Methocel F4M, HPMC and P407.

Raw material	D 0.1 ( $\mu\text{m}$ )	D 0.5 ( $\mu\text{m}$ )	D 0.9 ( $\mu\text{m}$ )	Span ( $\mu\text{m}$ )
CHD	5.14	21.00	69.00	3.04
HPMC	33.00	84.60	172.00	1.64
Methocel	26.50	70.80	202.00	2.48
P 407	11.50	34.50	74.30	1.82

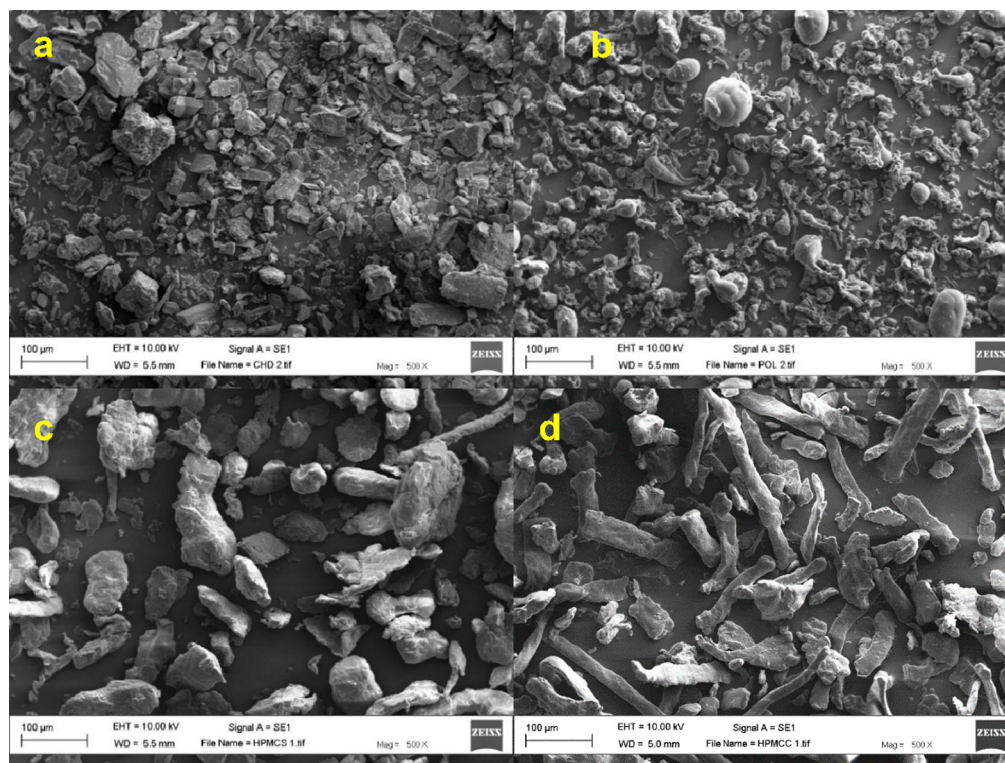


**Fig. 3.** SEM images of (a) CHD (b) P407, (c) HPMC and (d) Methocel x500.

**Table 4**  
Compressibility index (CI%) for tablet blends before and after granulation.

Formulations	Powder blends		Granules	
	CI%	Flow character	CI%	Flow character
F1	36.59 $\pm$ 4.00	Very poor	29.41 $\pm$ 1.03	Poor
F2	42.31 $\pm$ 1.61	Very, very poor	32.38 $\pm$ 1.58	Very poor
F3	42.86 $\pm$ 1.55	Very, very poor	32.29 $\pm$ 1.47	Very poor
F4	31.43 $\pm$ 2.91	Very poor	26.38 $\pm$ 0.00	Poor
F5	34.21 $\pm$ 3.62	Very poor	27.92 $\pm$ 0.92	Poor
F6	43.74 $\pm$ 1.32	Very, very poor	34.92 $\pm$ 1.37	Very poor
F7	39.28 $\pm$ 2.24	Very, very poor	34.85 $\pm$ 0.00	Very poor
F8	41.36 $\pm$ 2.12	Very, very poor	30.33 $\pm$ 3.21	Poor
F9	38.45 $\pm$ 4.43	Very, very poor	27.50 $\pm$ 0.87	Poor
F10	42.36 $\pm$ 5.81	Very, very poor	26.83 $\pm$ 0.76	Poor

brittle during manufacturing and handling. Furthermore, upon application, it promotes rapid hydration around the perimeter and facilitates adhesion (Foreman et al., 2006).

All tablets successfully adhered to the chicken crop when repeatedly immersed, using the disintegration tester, in the aqueous medium for two hours, which corresponds to the selected residence time for CHD release from the tablets in the buccal cavity. This successful mucoadhesion may be due to the chain entanglement and physical interlinking interaction of both the Hydroxypropyl methylcellulose polymers and the P407 with the chicken crop mucous membrane. Neither polymer is capable of interacting

with the mucin component of mucous as they are both uncharged (Sosnik et al., 2014).

### 3.6. Swelling index (SI) and tablet morphology

The swelling index for both Methocel and HPMC formulations (Fig. 5, supplemental data) increased with time. Statistical analysis (two-way ANOVA with replication) revealed no statistical significance ( $p > 0.05$ ) between HPMC and Methocel formulations (F1 and F6). This indicates that the morphology of HPMC and Methocel particles does not have any impact on the swelling index. However,

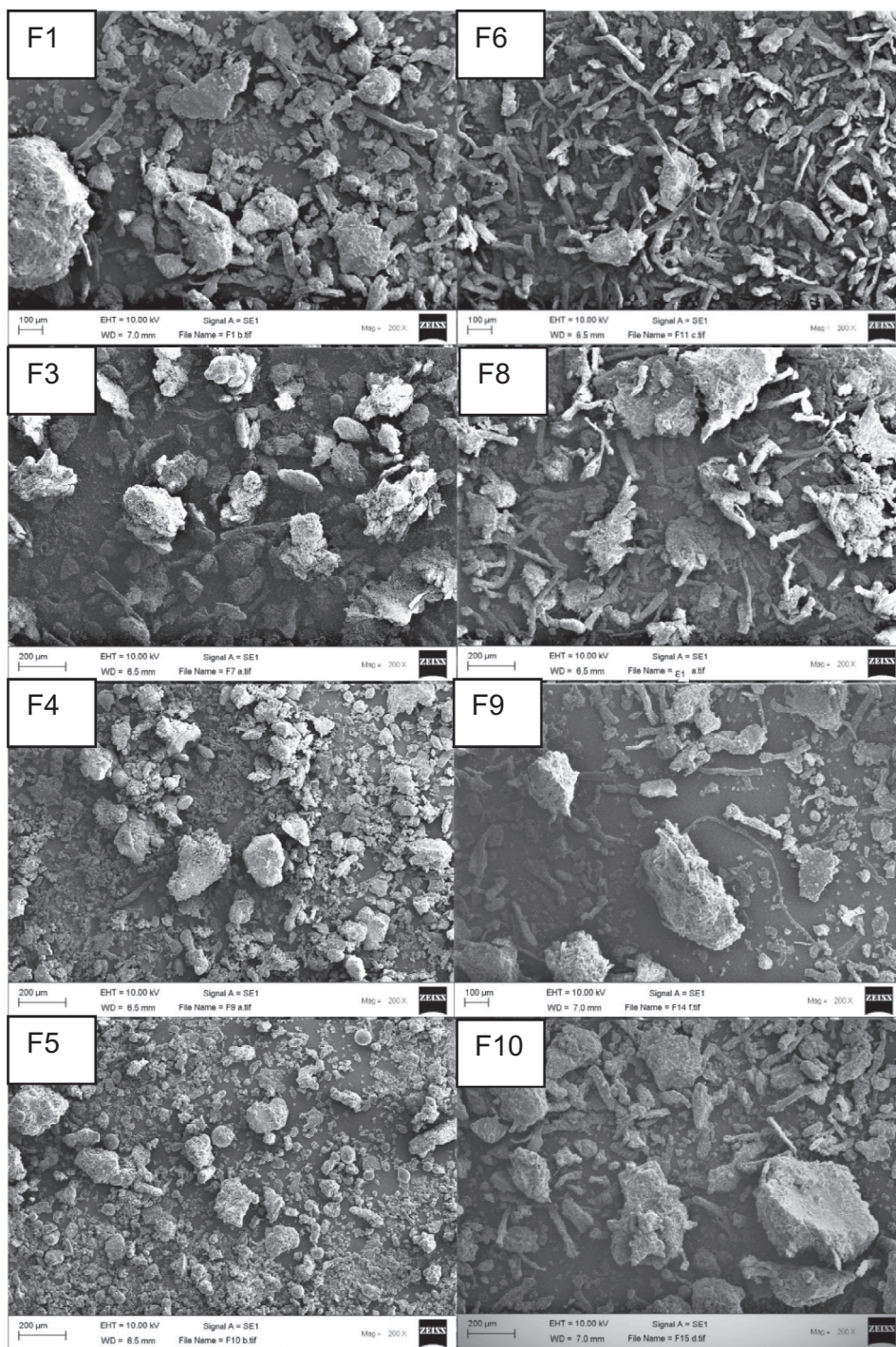


Fig. 4. SEM images of selected granules of HPMC and Methocel formulations, x200.

there was a significant difference for each group of formulations ( $p < 0.001$ ) for HPMC (F1 and F5) and Methocel (F6–F10).

Increasing P407 led to a significant decrease in the swelling index ( $p < 0.001$ ), for both HPMC formulations. Upon hydration, the mobility of the macromolecules in Methocel and HPMC increases along with the rate of water movement (Siepmann and Peppas, 2012). Moreover, hydrated P407 arranges itself into micellar structures that subsequently adopt a cubic shape once the hydrogel is formed. Intriguingly, the presence of HPMC in some of these formulations might facilitate the formation of a network of interconnected P407 micelles (Koffi et al., 2006).

SEM micrographs of swollen tablets (Fig. 6) show a sponge-like, porous network with a strong relationship between the shape of the pores and the morphology of the particles in Methocel and HPMC polymers (Fig. 3) and their ratios in the formulations. F1 and F2 show smaller and more spherical pores compared to F6, F7 and F8 which have elongated, larger pores. The effect is prominent when the ratio is greater than 50% in the tablet. For instance, the average cross-sectional surface area of the pores in F1 and F6 was  $0.46 \pm 0.86$  and  $1.86 \pm 2.95 \mu\text{m}^2$ , respectively. Although the average size of pores in F5 is  $\sim 4$  times that of F1, the total surface area of the pores was  $0.203 \text{ mm}^2$  for the former and  $0.234 \text{ mm}^2$  for

**Table 5**  
Tensile strength (n = 10) and friability (1 g) of CHD tablets.

Formulations	Tensile strength (MPa)	Friability (%)
F1	0.57 ± 0.19	0.48
F2	0.49 ± 0.19	0.28
F3	0.51 ± 0.14	0.12
F4	0.73 ± 0.21	0.09
F5	0.62 ± 0.15	0.36
F6	0.78 ± 0.14	0.04
F7	0.78 ± 0.18	0.02
F8	0.66 ± 0.21	0.01
F9	0.74 ± 0.28	0.06
F10	0.88 ± 0.20	0.25

the latter, with a ratio of 0.9. This indicates that although the size and the morphology of the pores are different, the total surface area is not greatly affected by the morphology of the polymeric particles. Increasing P407 leads to the formation of irregular pores, possibly because of its surfactant properties which increase the solubility of other polymers and distorts their shapes. Another possibility is that it might be affected by the thermosensitive properties of P407, which melts at a low temperature, meaning that pore damage may occur during the freeze-drying process or during the sample cutting of freeze-dried tablets.

### 3.7. In-vitro dissolution of CHD and data analysis

The cumulative CHD release from both groups of tablets was affected by the ratio of P407. Increasing P407 content elevates drug release by as much as 30% for HPMC formulations (F1 to F5). For example, 60.53% of CHD was released from F1 compared to 94.27% of CHD which was released from F5. Moreover, the cumulative CHD release from Methocel formulations F6 and F10 with the same composition as F1 and F5 were 57.77% and 94.58%, respectively. The increase in drug release was attributed to the solubilising activity of P407 (Fig. 7). The copolymer P407 is a surfactant which is widely used to improve the aqueous solubility of poorly soluble drugs (Dumortier et al., 2006), and can also form a hydrogel at body temperature. However, the morphology of the particles of Methocel and HPMC did not affect CHD release, which might be explained by the equivalent cross-sectional surface area of pores in F1 and F6. Moreover, both formulations are similar in terms of cumulative drug release based on similarity factor ( $f_2$ ) and difference factor ( $f_1$ ), with values of 81.1% and 6.87, respectively. F1 and F6 showed a cumulative release after two hours of 60.7% and 57.7%, while F5 and F10 showed 93.0% and 94.6%,

respectively. Both F5 and F10 can be considered similar with a  $f_2$  of 77.68% and a  $f_1$  of 6.36.

Although different compression forces of 10 KN for HPMC formulations and 40 KN for Methocel formulations were used to prepare the granules, this should not affect drug release. Velasco et al. (1999) reported that compression force has a minimal effect on drug release or the kinetics of release but can influence initial matrix porosity (before hydration).

The kinetics of CHD release was investigated by fitting the release data to the following models: zero order, first order, Higuchi, Hixson-Crowell and Korsmeyer-Peppas models (Table 2). Using the correlation coefficient ( $R^2$ ) values, the tablets fitted most closely with the Korsmeyer-Peppas kinetic model and the exponent  $n$  was found to be  $0.45 < n < 0.89$  (Table 6). This indicates that drug release is anomalous from cylindrical tablet (0.45 representing diffusional control and 0.89 indicating case-II transport which corresponds to zero order kinetic). Thus, CHD release is anomalous (Siepmann and Peppas, 2012). This leads to the conclusion that neither the morphology of polymer particles nor the ratio of P407 had an effect on the mechanism of drug release.

### 3.8. Drug polymer interaction (FTIR and DSC)

The FTIR spectra revealed that HPMC and Methocel are identical in terms of chemical composition. Moreover, analyses were performed (Fig. 8) to evaluate possible interactions during the granulation and tableting process which might have resulted from the low melting point of P407. CHD displayed peaks at 3325 and 3119  $\text{cm}^{-1}$  (asymmetric and symmetric NH stretching vibrations), 2938 and 2886  $\text{cm}^{-1}$  (asymmetric and symmetric CH stretching), 1624  $\text{cm}^{-1}$  (CN stretching vibration of imine group), 1522, 1483  $\text{cm}^{-1}$  (NH bending vibration of secondary amine and imine groups), 1406  $\text{cm}^{-1}$  (C=C stretching vibrations of aromatic rings), 1290 and 1245  $\text{cm}^{-1}$  CN stretching, 819  $\text{cm}^{-1}$  (out of plane vibration of the aromatic ring and the CCl group's spectra at 718  $\text{cm}^{-1}$  (Holešová et al., 2014, and Yang et al., 2007). The characteristic peaks of HPMC are at 3445  $\text{cm}^{-1}$  (OH stretching) and 2897  $\text{cm}^{-1}$  (CH stretching), 1375  $\text{cm}^{-1}$  (asymmetric  $\text{CH}_3$  bending vibration), 1049  $\text{cm}^{-1}$  (C–O asymmetric stretching vibration) and 942  $\text{cm}^{-1}$  (C–O symmetric stretching vibration (Ding et al., 2015). P407 is characterised by principal peaks at 2875  $\text{cm}^{-1}$  (CH stretching), 1346  $\text{cm}^{-1}$  (OH bending) and 1094  $\text{cm}^{-1}$  (CO stretching) (Vyas et al., 2009). The analyses of tablet formulations (Fig. 8 a and c) reveal that increasing the concentration of P407 leads to a decreased intensity of CHD and the disappearance of hydrogen bonding peaks at 3325 and 3119  $\text{cm}^{-1}$ . This is prominent in F5 and F10. In contrast, F1, F2, F6 and F7 show a combination of the

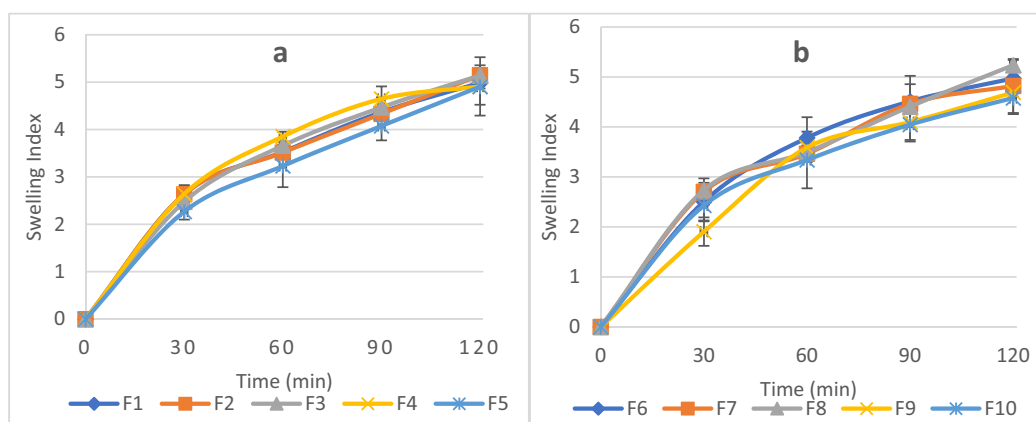


**Fig. 5.** swelling index of CHD tablets (a) HPMC formulations and (b) Methocel formulations in ultrapure water and at 37 °C, Data are expressed as mean ± SD, n = 3.

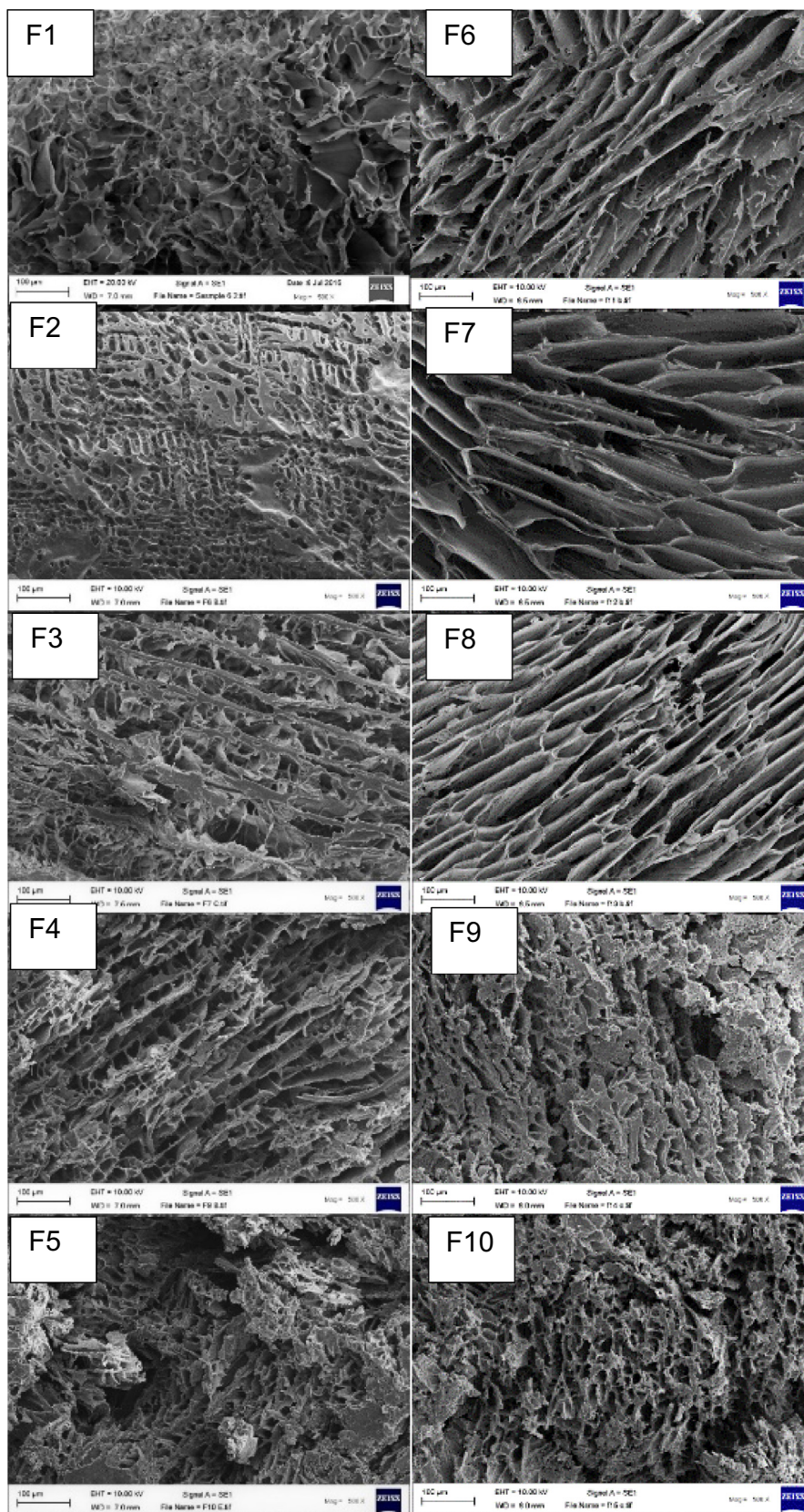


Fig. 6. SEM micrographs of cross-section of freeze-dried swollen tablets.

peaks of all ingredients. The concentration-dependent interaction between CHD and P407 is attributed to the steric hindrance properties of P407, resulting in the shielding of CHD (Göppert and

Müller, 2005). The peaks of HPMC overlap with those of P407, with the CO stretching of HPMC, Methocel and P407 combining into one peak at around  $1097\text{ cm}^{-1}$  in F2, F8 and F5 and F8-F10. However, in



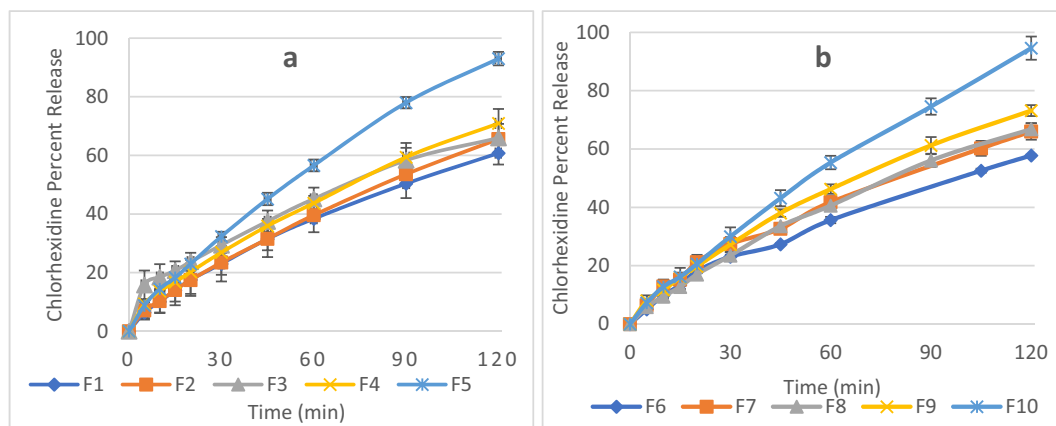


Fig. 7. Cumulative percentage release of CHD from (a) HPMC formulations and (b) Methocel formulations in ultrapure water at  $37 \pm 0.1$  °C and 50 rpm,  $n = 3 \pm SD$ .

**Table 6**  
CHD release kinetics using different models.

	Zero Order ( $R^2$ )	First order ( $R^2$ )	Higuchi ( $R^2$ )	Hixon crowel ( $R^2$ )	K-Peppas ( $R^2$ )	K-Peppas (n)
F1	$0.9702 \pm 0.0227$	$0.9826 \pm 0.0149$	$0.9723 \pm 0.0262$	$0.9697 \pm 0.0285$	$0.9979 \pm 0.0010$	$0.717 \pm 0.139$
F2	$0.9795 \pm 0.0143$	$0.9825 \pm 0.0078$	$0.9655 \pm 0.0244$	$0.9757 \pm 0.0188$	$0.9967 \pm 0.0023$	$0.747 \pm 0.137$
F3	$0.9329 \pm 0.0378$	$0.8943 \pm 0.0843$	$0.9818 \pm 0.0063$	$0.8567 \pm 0.1076$	$0.9872 \pm 0.0029$	$0.541 \pm 0.105$
F4	$0.9776 \pm 0.0028$	$0.9867 \pm 0.0078$	$0.9773 \pm 0.0031$	$0.9777 \pm 0.0130$	$0.9985 \pm 0.0008$	$0.686 \pm 0.027$
F5	$0.9850 \pm 0.0048$	$0.9806 \pm 0.0035$	$0.9648 \pm 0.0050$	$0.9940 \pm 0.0014$	$0.9984 \pm 0.0012$	$0.764 \pm 0.029$
F6	$0.9712 \pm 0.0054$	$0.9833 \pm 0.0067$	$0.9736 \pm 0.0063$	$0.9483 \pm 0.0128$	$0.9965 \pm 0.0007$	$0.698 \pm 0.033$
F7	$0.9663 \pm 0.0025$	$0.9854 \pm 0.0028$	$0.9796 \pm 0.0019$	$0.9714 \pm 0.0042$	$0.9959 \pm 0.0005$	$0.671 \pm 0.018$
F8	$0.9791 \pm 0.0107$	$0.9972 \pm 0.0010$	$0.9606 \pm 0.0071$	$0.9942 \pm 0.0030$	$0.9983 \pm 0.0015$	$0.796 \pm 0.009$
F9	$0.9727 \pm 0.0117$	$0.9952 \pm 0.0012$	$0.9703 \pm 0.0105$	$0.9894 \pm 0.0081$	$0.9981 \pm 0.0015$	$0.740 \pm 0.044$
F10	$0.9907 \pm 0.0079$	$0.9700 \pm 0.0143$	$0.9475 \pm 0.0190$	$0.9872 \pm 0.0059$	$0.9987 \pm 0.0005$	$0.870 \pm 0.113$

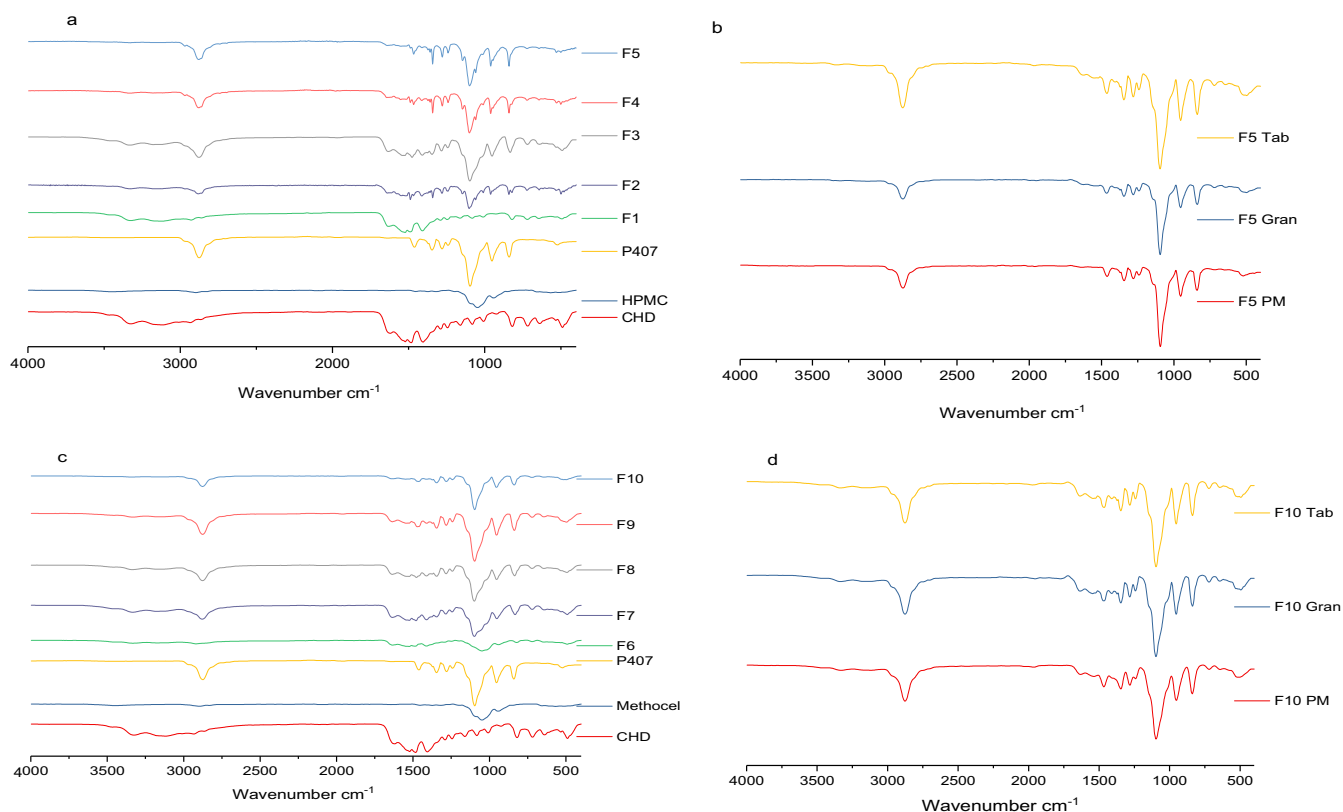


Fig. 8. FTIR spectra of (a) HPMC formulations, (b) F5 physical mix (PM), granules (Gran) and tablet (Tab), (c) Methocel formulations and (d) F10 PM, Gran and Tab.

F1 and F6, this peak shifts to  $1049\text{ cm}^{-1}$ . Further investigation was performed to analyse F5 and F10, the physical mix, the granules and the tablets (Fig. 8 b and d). All FTIR spectra have identical peaks, meaning that during the mixing process of the excipient, hydrophobic interactions occur between CHD and P407 ending in steric hindrance by the latter. Although this interaction is more common in liquid formulations, in the current formulation the interaction is aggravated by the small particle size of both CHD and P407.

Fig. 9 shows the DSC thermograms for raw materials, the physical mixture, the granules and the tablet of F10 formulation, which has the highest drug release. CHD has two melting peaks at  $158$  and  $176^\circ\text{C}$ , which indicates its polymorphic nature. Methocel reflects its amorphous nature while P407 has a melting peak at  $57^\circ\text{C}$ . The F10 physical mix, the granules and the tablet thermograms showed that the endothermic peak of poloxamer occurred at around the same temperature. The first melting peak of CHD was shifted to  $156^\circ\text{C}$  in the physical mix and to  $153^\circ\text{C}$  in the granules and the compressed tablet. The small melting peak disappeared in the physical mix and granules but in the tablet, it shifted to  $173^\circ\text{C}$ . The shifting and the disappearance of the melting peaks in the physical mix and the granules indicate there is an interaction between the chlorhexidine and the P407. However, the re-appearance of the second endothermic peak in the tablet is attributed to phase separation resulting from tablet compression (Singh et al., 2016).

The interaction between the excipients and CHD were tested using FTIR and DSC. The FTIR spectra revealed that increases in the ratio of P407 led to a decrease in the intensity of CHD which can be attributed to steric hindrance by P407. The FTIR spectra

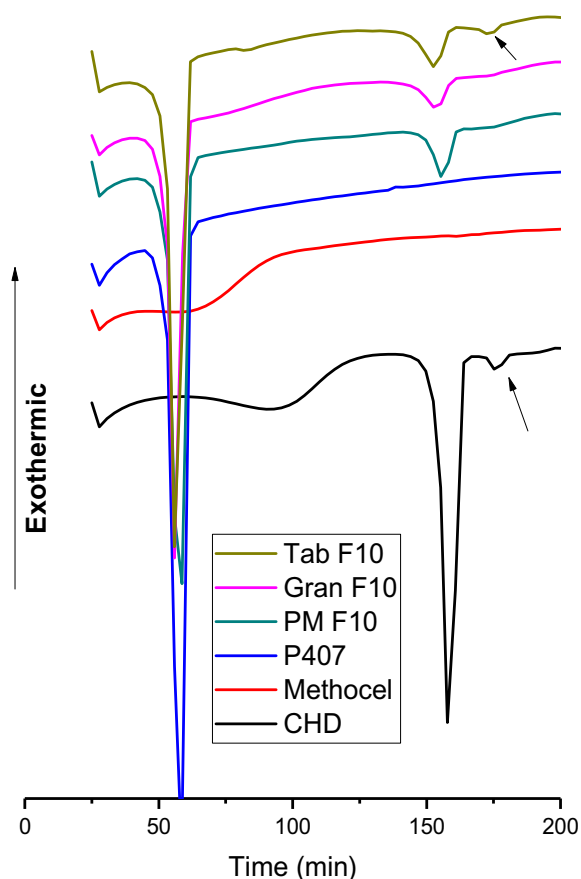


Fig. 9. DSC thermograms of F10 physical mix (PM), Granules (GRAN), tablet (TAB), CHD, Methocel and P407.

for the F5 physical mix, the granules and the tablet showed identical spectra with that of the F10. This indicates that no interaction occurred during the process of tableting and the sources of the polymer showed no differences in behaviour. Moreover, DSC analysis was performed on the F10 formulation only and showed no interactions between the drug and the polymers in the prepared table.

#### 4. Conclusions

CHD buccal tablets were successfully prepared using two different sources of hydroxypropyl methylcellulose polymer. Both groups of formulations showed comparable drug release and kinetics of drug release. The addition of the thermosensitive hydrogel-forming polymer P407 to the formulations improved CHD release from the tablets without negatively impacting on the duration of mucoadhesion. *In vivo* work will be undertaken in the future to further investigate the safety and efficacy of the prepared buccal tablets for future application in the treatment of OPC.

#### Appendix A. Supplementary material

Supplementary data to this article can be found online at <https://doi.org/10.1016/j.jpsps.2019.04.012>.

#### References

- Ankola, A.V., Hebbal, M., Mocherla, M., 2008. A review of efficacy of various modes of chlorhexidine delivery. *J. Oral Biosci.* 50, 239–242. [https://doi.org/10.1016/S1349-0079\(08\)80013-8](https://doi.org/10.1016/S1349-0079(08)80013-8).
- British Pharmacopoeia Commission, 2017. Appendix XVII N. Powder Flow1 - British Pharmacopoeia [WWW Document]. URL <https://www.pharmacopoeia-com.ezproxy.wlv.ac.uk/bp-2014/appendices/appendix-17/appendix-xvii-n-powder-flow1.html?date=2014-01-01&text=Powder+Flow> (accessed 12.2.18).
- Costa, P., Lobo, J.M.S., 2001. Modelling and comparison of dissolution profiles. *Eur. J. Pharm. Sci.* 13, 123–133. [https://doi.org/10.1016/S0928-0987\(01\)00095-1](https://doi.org/10.1016/S0928-0987(01)00095-1).
- Ding, C., Zhang, M., Li, G., 2015. Preparation and characterization of collagen/hydroxypropyl methylcellulose (HPMC) blend film. *Carbohydr. Polym.* 119, 194–201. <https://doi.org/10.1016/j.carbpol.2014.11.057>.
- Dumortier, G., Grossiord, J.L., Agnely, F., 2006. A review of poloxamer 407 pharmaceutical and pharmacological characteristics. *Pharm. Res.* 23, 2709–2728. <https://doi.org/10.1007/s11095-006-9104-4>.
- Elena Campos-Aldrete, M., 1997. Influence of the viscosity grade and the particle size of HPMC on metronidazole release from matrix tablets. *Eur. J. Pharm. Biopharm.*
- Foreman, P., Zhang, Y., Puri, R., 2006. Mucosal delivery tablet. US 2007/0048369 A1.
- Gao, P., Skoug, J.W., Nixon, P.R., Robert Ju, T., Stemm, N.L., Sung, K.-C., 1996. Swelling of hydroxypropyl methylcellulose matrix tablets. 2. Mechanistic study of the influence of formulation variables on matrix performance and drug release. *J. Pharm. Sci.* 85, 732–740. <https://doi.org/10.1021/js9504595>.
- Garg, V., Mallick, S.S., Garcia-Trinanes, P., Berry, R.J., 2018. An investigation into the flowability of fine powders used in pharmaceutical industries. *Powder Technol.* 336, 375–382. <https://doi.org/10.1016/J.POWTEC.2018.06.014>.
- Ghori, M.U., Conway, B.R., 2015. Hydrophilic matrices for oral control drug delivery. *Am. J. Pharmacol. Sci.* 3, 103–109. <https://doi.org/10.12691/AJPS-3-5-1>.
- Göppert, T.M., Müller, R.H., 2005. Protein adsorption patterns on poloxamer- and poloxamine-stabilized solid lipid nanoparticles (SLN). *Eur. J. Pharm. Biopharm.* 60, 361–372. <https://doi.org/10.1016/j.ejpb.2005.02.006>.
- Gustafsson, C., Bonferoni, M.C., Caramella, C., Lennholm, H., Nyström, C., 1999. Characterisation of particle properties and compaction behaviour of hydroxypropyl methylcellulose with different degrees of methoxy/hydroxypropyl substitution. *Eur. J. Pharm. Sci.* 9, 171–184. [https://doi.org/10.1016/S0928-0987\(99\)00054-8](https://doi.org/10.1016/S0928-0987(99)00054-8).
- Gustafsson, C., Nyström, C., Lennholm, H., Bonferoni, M.C., Caramella, C.M., 2003. Characteristics of hydroxypropyl methylcellulose influencing compactibility and prediction of particle and tablet properties by infrared spectroscopy. *J. Pharm. Sci.* 92, 494–504. <https://doi.org/10.1002/jps.10323>.
- Hassan, M.S., Lau, R.W.M., 2009. Effect of particle shape on dry particle inhalation: study of flowability, aerosolization, and deposition properties. *AAPS PharmSciTech* 10, 1252–1262. <https://doi.org/10.1208/s12249-009-9313-3>.
- Herting, M.G., Kleinebudde, P., 2007. Roll compaction/dry granulation: effect of raw material particle size on granule and tablet properties. *Int. J. Pharm.* 338, 110–118. <https://doi.org/10.1016/j.ijpharm.2007.01.035>.
- Holešová, S., Valášková, M., Hlaváč, D., Madejová, J., Samlíková, M., Tokarský, J., Pazziora, E., 2014. Antibacterial kaolinite/urea/chlorhexidine nanocomposites:

- experiment and molecular modelling. *Appl. Surf. Sci.* 305, 783–791. <https://doi.org/10.1016/j.apsusc.2014.04.008>.
- Kabanov, A.V., Batrakova, E.V., Alakhov, V.Y., 2002. P luronic block copolymers for overcoming drug resistance in cancer. *Adv. Drug Deliv. Rev.*
- Kassem, M.A.A., Elmehad, A.N., Fares, A.R., 2014. Enhanced bioavailability of buspirone hydrochloride via cup and core buccal tablets: formulation and in vitro/in vivo evaluation. *Int. J. Pharm.* 463, 68–80. <https://doi.org/10.1016/j.ijpharm.2014.01.003>.
- Koffi, A.A., Agnely, F., Ponchel, G., Grossiord, J.L., 2006. Modulation of the rheological and mucoadhesive properties of thermosensitive poloxamer-based hydrogels intended for the rectal administration of quinine. *Eur. J. Pharm. Sci.* 27, 328–335. <https://doi.org/10.1016/j.ejps.2005.11.001>.
- Li, C.L., Martini, L.G., Ford, J.L., Roberts, M., 2005. The use of hypromellose in oral drug delivery. *J. Pharm. Pharmacol.* 57, 533–546. <https://doi.org/10.1211/0022357055957>.
- Lim, K.S., Kam, P.C.A., 2008. Chlorhexidine – pharmacology and clinical applications. *Anaesth. Intensive Care* 36, 502–512. [https://doi.org/10.1016/S0140-6736\(08\)60601-7](https://doi.org/10.1016/S0140-6736(08)60601-7). *Anaesthesia*.
- Liu, L.X., Marziano, I., Bentham, A.C., Litster, J.D., White, E.T., Howes, T., 2008. Effect of particle properties on the flowability of ibuprofen powders. *Int. J. Pharm.* 362, 109–117. <https://doi.org/10.1016/j.ijpharm.2008.06.023>.
- Maderuelo, C., Zarzuelo, A., Lanao, J.M., 2011. Critical factors in the release of drugs from sustained release hydrophilic matrices. *J. Control. Release* 154, 2–19. <https://doi.org/10.1016/j.jconrel.2011.04.002>.
- Matanovi, M.R., Kristl, J., Grabnar, A., 2014. Thermoresponsive polymers: Insights into decisive hydrogel characteristics, mechanisms of gelation, and promising biomedical applications. *Int. J. Pharm.* 472, 262–275. <https://doi.org/10.1016/j.ijpharm.2014.06.029>.
- Maurya, S., Pathak, K., Bali, V., 2010. Therapeutic potential of mucoadhesive drug delivery systems – an updated patent review. *Recent Pat. Drug Deliv. Formul.* 4, 256–265. <https://doi.org/10.2174/187221110793237529>.
- Nafee, N.A., Ismail, F.A., Boraie, N.A., Mortada, L.M., 2003. Mucoadhesive buccal patches of miconazole nitrate: In vitro/in vivo performance and effect of ageing. *Int. J. Pharm.* 264, 1–14. [https://doi.org/10.1016/S0378-5173\(03\)00371-5](https://doi.org/10.1016/S0378-5173(03)00371-5).
- Naito, M., Hayakawa, O., Nakahira, K., Mori, H., Tsubaki, J., 1998. Effect of particle shape on the particle size distribution measured with commercial equipment. *Powder Technol.* 100, 52–60. [https://doi.org/10.1016/S0032-5910\(98\)00052-7](https://doi.org/10.1016/S0032-5910(98)00052-7).
- Pereiro Ferreirós, M., García-Martínez, F.J., Alonso-González, J., 2012. Update on the treatment of superficial mycoses. *Actas Dermosifiliogr.* 103, 778–783. <https://doi.org/10.1016/j.ad.2012.01.009>.
- Pitt, K.G., Newton, J.M., Stanley, P., 1988. Tensile fracture of doubly-convex cylindrical discs under diametral loading. *J. Mater. Sci.* 23, 2723–2728. <https://doi.org/10.1007/BF00547442>.
- Rohrs, B.R., 2001. Dissolution method development for poorly soluble compounds. *Dissolution Technol.* 29, 1171–1178. <https://doi.org/10.14227/DT080301P6>.
- Ruel-Gariépy, E., Leroux, J.C., 2004. In situ-forming hydrogels – review of temperature-sensitive systems. *Eur. J. Pharm. Biopharm.* 58, 409–426. <https://doi.org/10.1016/j.ejpb.2004.03.019>.
- Sankar, V., Hearnden, V., Hull, K., Juras, D.V., Greenberg, M., Kerr, A., Lockhart, P., Patton, L., Porter, S., Thornhill, M., 2011. Local drug delivery for oral mucosal diseases: challenges and opportunities. *Oral Dis.* 17, 73–84. <https://doi.org/10.1111/j.1601-0825.2011.01793.x>.
- Siepmann, J., Peppas, N.A., 2012. Modeling of drug release from delivery systems based on hydroxypropyl methylcellulose (HPMC). *Adv. Drug Deliv. Rev.* 64, 163–174. <https://doi.org/10.1016/j.addr.2012.09.028>.
- Singh, A., Bharati, A., Frederiks, P., Verkinderen, O., Goderis, B., Cardinaels, R., Moldenaers, P., Van Humbeeck, J., Van Den Mooter, G., 2016. Effect of compression on the molecular arrangement of itraconazole-soluplus solid dispersions: induction of liquid crystals or exacerbation of phase separation? *Mol. Pharm.* 13, 1879–1893. <https://doi.org/10.1021/acs.molpharmaceut.6b00046>.
- Sosnik, A., Das Neves, J., Sarmento, B., 2014. Mucoadhesive polymers in the design of nano-drug delivery systems for administration by non-parenteral routes: a review. *Prog. Polym. Sci.* 39, 2030–2075. <https://doi.org/10.1016/j.progpolymsci.2014.07.010>.
- Sudhakar, Y., Kuotsu, K., Bandyopadhyay, A.K., 2006. Buccal bioadhesive drug delivery – a promising option for orally less efficient drugs. *J. Control. Release*. <https://doi.org/10.1016/j.jconrel.2006.04.012>.
- Tuğcu-Demiröz, F., Acartürk, F., Takka, S., Konuş-Boyunağa, Ö., 2004. In-vitro and in-vivo evaluation of mesalazine-guar gum matrix tablets for colonic drug delivery. *J. Drug Target.* 12, 105–112. <https://doi.org/10.1080/10611860410001693751>.
- Velasco, M.V., Ford, J.L., Rowe, P., Rajabi-Siahboomi, A.R., 1999. Influence of drug: hydroxypropylmethylcellulose ratio, drug and polymer particle size and compression force on the release of diclofenac sodium from HPMC tablets. *J. Control. Release* 57, 75–85. [https://doi.org/10.1016/S0168-3659\(98\)00110-2](https://doi.org/10.1016/S0168-3659(98)00110-2).
- Vyas, V., Sancheti, P., Karekar, P., Shah, M., Pore, Y., 2009. Physicochemical characterization of solid dispersion systems of tadalafil with poloxamer 407. *Acta Pharm.* 59, 453–461. <https://doi.org/10.2478/v10007-009-0037-4>.
- Wan, P., Heng, S., Chan, L.W., Easterbrook, M.G., Li, X., 2001. Investigation of the influence of mean HPMC particle size and number of polymer particles on the release of aspirin from swellable hydrophilic matrix tablets. *J. Controlled Release*.
- Xie, T., Gao, W., Taylor, L.S., 2017. Impact of Eudragit EPO and hydroxypropyl methylcellulose on drug release rate, supersaturation, precipitation outcome and redissolution rate of indomethacin amorphous solid dispersions. *Int. J. Pharm.* 531, 313–323. <https://doi.org/10.1016/j.ijpharm.2017.08.099>.
- Yang, D., Yuan, P., Zhu, J.X., He, H.P., 2007. Synthesis and characterization of antibacterial compounds using montmorillonite and chlorhexidine acetate. *J. Therm. Anal. Calorim.* 89, 847–852. <https://doi.org/10.1007/s10973-006-8318-3>.